





## TLM MODELLING OF A SLOTTED WEARABLE MICROSTRIP ANTENNA UNDER BENDING CONDITIONS\*

Jugoslav J. Joković<sup>1</sup>, Tijana Ž. Dimitrijević<sup>1,2</sup>,  
Aleksandar S. Atanasković<sup>1</sup>, Nebojša S. Dončov<sup>1</sup>

<sup>1</sup>Faculty of Electronic Engineering, University of Niš, Republic of Serbia

<sup>2</sup>Faculty of Engineering, University of Kragujevac, Republic of Serbia

ORCID iDs:	Jugoslav J. Joković	 <a href="https://orcid.org/0000-0002-4780-938X">https://orcid.org/0000-0002-4780-938X</a>
	Tijana Ž. Dimitrijević	 <a href="https://orcid.org/0000-0002-9744-8287">https://orcid.org/0000-0002-9744-8287</a>
	Aleksandar S. Atanasković	 <a href="https://orcid.org/0000-0002-9979-5995">https://orcid.org/0000-0002-9979-5995</a>
	Nebojša S. Dončov	 <a href="https://orcid.org/0000-0002-9057-6737">https://orcid.org/0000-0002-9057-6737</a>

**Abstract.** *This paper investigates the potential of the Transmission Line Matrix (TLM) method and highlights the efficiency of a conformal cylindrical mesh for analyzing the tunable capabilities of a wearable slotted antenna under bending conditions. Various configurations of polygon-shaped and U-shaped slots inserted into the radiating patch of a rectangular antenna are considered to illustrate their tuning effects on antenna parameters. The cylindrical TLM approach is demonstrated to be particularly effective for the efficient and accurate analysis of a flexible slotted antenna attached to the human body, focusing on resonant frequencies and reflection coefficients under different bending angles. The simulated results confirm the consistency of frequency shifts caused by bending, while the cylindrical mesh provides precise analysis of the impact of slot shape and size on antenna performance.*

**Key words:** *slotted antenna, wearable antennas, antenna bending, transmission line modelling method*

### 1. INTRODUCTION

Wearable patch antennas represent basic components in systems for communication between a human body and the external world. Integrating these antennas into fabrics enhances user safety, convenience, and operability, making them valuable in applications related to health monitoring and personal communications, including both on-body and off-body solutions [2,3]. Different microstrip patch configurations and textile materials

---

Received August 23, 2024; revised November 29, 2024 and July 17, 2025; accepted July 17, 2025

**Corresponding author:** Jugoslav Joković

Faculty of Electronic Engineering, University of Niš, Aleksandra Medvedeva 4, Niš, Serbia

E-mail: jugoslav.jokovic@elfak.ni.ac.rs

\*An earlier version of this paper was presented at the 16th International Conference on Advanced Technologies, Systems and Services in Telecommunications (TELSIKS 2023), October 25-27, 2023, Niš, Serbia [1]

were analysed and used to design and test the wearable antennas [4-7]. Inserting differently shaped slots onto a radiated surface of a rectangular patch can improve antenna performances in terms of circular polarization, wideband and/or dual band use in many communication systems, such as space and military personal communications, fire-fighting, and rescue work [6-10].

Generally, for on-body wearable electronic applications the main challenge is related to a flexibility of an antenna deployed on different parts on a human body (on-body antennas), either embedded into a human skin (implantable antennas) or clothing (textile antennas). Since the antenna attached on the body will easily bend due to the human body structure and movement, details of the antenna parameter variations under the bending condition should be considered [2,3,11]. However, there are many challenges in antenna design arising from the close proximity of the human body, variations of the human body posture, and motions in everyday activities. Due to interference effects between the body and the deformed antenna, many antenna parameters, such as resonant frequency, gain, radiation pattern, and polarization, could change. A trade-off between flexibility and performance stability under deformation and mutual interference has a great importance in providing a correct functioning of the antenna: the frequency and return loss in operating bands must be compliant with specifications, stable and predictable under deformations, and interference effect of components in close proximity to the antenna.

To address these challenges, different types of numerical models of wearable antennas are usually used in design and testing. Various tools based on full-wave numerical techniques such as Finite-Difference Time-Domain – FDTD [12], Method of Moments – MoM [13], Finite Element Method – FEM [14], Transmission Line Matrix - TLM [15], can be used to study antenna parameters by generating geometrical models of antennas while taking into account dielectric characteristics of textile materials and human body tissues. Advantages and disadvantageous of these methods have been reported so far showing their differences with respect to memory requirement and run-time, their modifications (e.g. from one domain to another) and enhancements (e.g. compact models). However, in general the choice of most optimal method depends on the nature of EM problem that needs to be solved. In contrast to MoM and FEM that are integral frequency-domain methods, the FDTD and TLM belongs to the class of differential time-domain methods that are most suited for solving closed-boundary EM problems. Although FDTD method is more well-known, the TLM method offers some crucial advantages in certain complex problems. The EM fields are co-located at the center of the TLM cell, making the TLM more naturally suited to the simulation of materials with different characteristics (including anisotropy). In addition, for the simulation of complex geometries, the mesh layout is simpler in the TLM method. It is also possible to operate on the EM fields on the boundaries of the cell and it is straightforward, for example, to apply impedance boundary conditions. The TLM method based on rectangular grid have been applied to antenna design in various configurations, from simple rectangular patch on different substrates, to complex meander-lined design [16-18].

The TLM method based on cylindrical coordinates [19,20] is highlighted for its ability to accurately and efficiently model cylindrically bent antennas, providing fully conformal analyses of bending deformation [21,22]. Advantages of this approach when it comes to modelling of bent antennas, with respect to the rectangular TLM approach that uses staircase approximation to represent curved surfaces, are demonstrated on the example of the rectangular patch antenna in [11]. A possibility of an accurate analysis of

the bending influence without approximating the radiated surface, using the same mesh regardless of the bending angle, is particularly highlighted. Separating the bending influence from the influence of different mesh resolutions is crucial, as it prevents alterations in the radiated surface size, substrate thickness, coaxial feed position, and other factors important in the antenna design.

Antennas based on slotted patch configurations offer broadband and/or multi-band tunable capabilities, making them advantageous over traditional antennas without slots. However, designing slotted patch antennas involves complex considerations due to their nonlinear and frequently non-unique nature, and, therefore time consuming procedures have to be used. The theory and design rules are not simple; they can be based on mathematics, and/or can be synthesized from experiments and physical insight, as well as from detailed numerical analyses. With using these mechanisms, the different shape slots can be synthesized and give satisfied results in terms of antenna performance improving [4-10]. However, this complexity necessitates precise modeling and intricate design rules, as small changes in slot dimensions can significantly affect antenna parameters. Simulations using methods like FDTD show that the slotted antenna is frequency-reconfigurable capable of shifting its operating frequency depending of slot dimension, with the radiation pattern essentially unaffected by the frequency tuning [5]. The analysis of circularly polarized patch antennas, configurations with U-slot and E-slot, have confirmed the modifications of these two antennas with optimal position and size of slot configuration affects to better axial ratio and cross-polarization performance compared to conventional antenna design [6]. In addition, a wideband patch antenna can be designed for dual- and multi-band application by cutting U-slots on the patch [7]. Also, by optimizing the E-slot length, width, and position, a wide-band mechanism with more than 30% bandwidth of single-patch antenna can be provided [8]. The configuration based on polygon shaped slot incorporated in rectangular patch is used for dual-band satellite applications like Iridium and GPS, with potential integration of the developed antenna solution into clothing [9]. As a result, if the rectangular mesh is used for modelling of the slotted wearable antenna the mesh resolution would be significantly increased in order to meet specific physical solution requirements that include keeping the constant slot dimension and position under different bending angles. The required simulation time may be reduced, if a model can be found to provide initial solution which is adaptive to the different situation in terms of bending. However, the set of effective parameters for adjustments in the model has to be small to ensure rapid iteration and conformal analyses. Understanding and applying these principles can help in modelling of slotted patch antennas that meet specific performance requirements under bending while managing model complexity and design cost.

This paper focuses on possibilities of the cylindrical TLM method to analyze a textile bent antenna with different shapes of slots inserted into the radiated patch. Two models of the rectangular patch antenna containing polygon-shaped and U-shaped slots of varying dimensions within the radiated patch which is placed on a human tissue are considered, as presented in Fig.1. The antenna model with the octagon-shaped slots that has been already presented in [1] is extended introducing U-shaped slot configuration. The paper provides more detailed analysis of results in terms of simultaneous considering both the influence of different slot size and the influence of different bending angle to antenna parameters. This paper also explains all the issues relevant to the cylindrical mesh used for the modelling which is crucial in ensuring reliable results. For verification

purpose, results of the flat antenna are compared with corresponding results obtained by the rectangular mesh, for both considered slot configurations.

## 2. TLM MODEL OF WEARABLE SLOTTED ANTENNA UNDER BENDING

The TLM numerical method is used to model wearable slotted antennas with the possibility of bending over the cylinder. This method, which is generally convenient for solving different electromagnetic (EM) problems in the time-domain, uses the equivalences between Maxwell's equations and the voltages and currents propagation along transmission lines. EM wave propagation is modelled by using a network of interconnected nodes, while taking into account discontinuities and interactions with different materials [15].

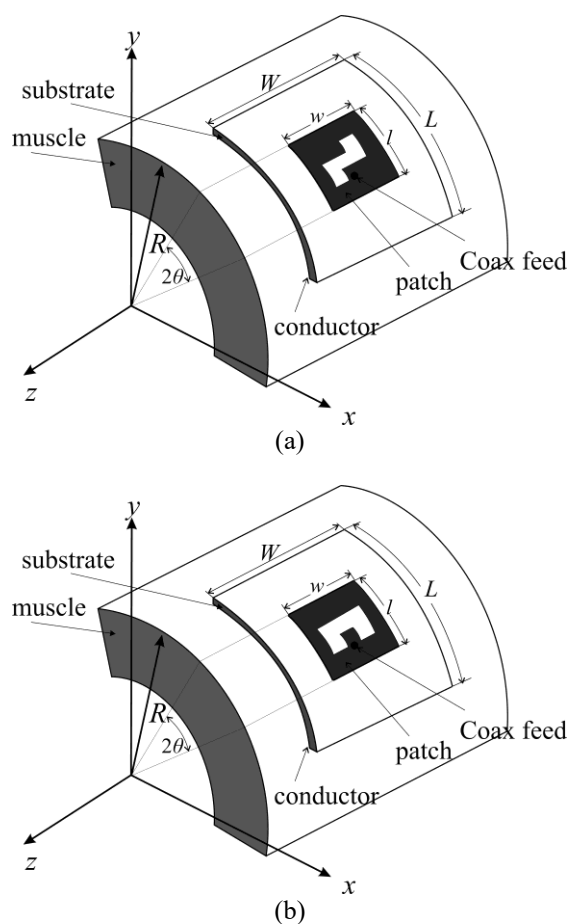


**Fig.1** A wearable antenna with an: (a) octagon-shaped slot [1], (b) U-shaped slot

While the TLM method was initially developed in a Cartesian grid [15], it has been found that for structures containing cylindrical or circular surfaces, the TLM method based on the cylindrical mesh is more convenient and efficient [19-23]. Adaptation of the TLM method to the cylindrical grid requested two main iterative procedures of the TLM algorithm: scattering and connection, to be adjusted to the orthogonal polar mesh and to be modified to account for excitation, boundaries, and inhomogeneous medium and losses [19,20,23]. The capability and computational efficiency of the TLM method, using a compact wire model aligned with the axial direction of the cylindrical grid, are demonstrated in the case of a coaxially fed patch-ring antenna [20]. Further adaptation included implementation of the compact wire model [18,21,22] facilitating the representation of the wires placed along a radial direction which enabled, for instance, modeling of a coaxial feed placed along the radial direction, as it is the case with a rectangular patch antenna bent over a cylinder investigating here [21,22]. This required appropriate adjustments to the connection procedure in form of an additional connecting procedure for wire segments located along a radial direction, where impedances of link and stub lines, embedded into the mesh to account for the wire, are different for neighboring nodes [21,22].

When a wearable antenna model having a possibility of bending over a cylinder is considered, a computational box should be defined as a part of cylinder rather than a whole cylinder to reduce memory requirements. Note that the patch antenna dimensions are much smaller than the radius of the surrounding cylinder defined via the bending angle, meaning that the antenna is located far away from the center of the cylinder, so the usage of the whole cylinder as the computational box would be a memory consuming. To address this, the TLM algorithm was adjusted to allow for setting up boundary conditions along the angular directions, enabling a more efficient representation of the modeling space as a part of a cylinder. This adjustment also involved defining the boundary condition on the inner surface of the computational box along the radial direction, instead of defining the central node which must be used in the case of a completely cylindrically shaped computational box. This adaptation has allowed for more efficient modeling of the wearable antenna which can bent over a cylinder [21,22].

The TLM model of the wearable antenna implies description of the metallic layers of the antenna, the radiated patch and the ground plane, as the perfect electrical conductor (PEC). In case of the radiated patch containing slots the cells representing slots should be excluded from the boundary conditions. This allows for the exchange of pulses with neighboring cells between the upper side of the substrate and the space above the antenna. To maintain a constant surface value of metallic parts and slots when the antenna is bent, which directly affects the antenna resonant frequency, a mesh resolution in the angular direction of individual regions is fine-tuned depending on the bending angle. This ensures consistency in sense that the number of cells in the specific region remains unchanged regardless of the bending angle, enabling accurate representation of the slotted antenna dimensions and reliable analysis under the bending conditions.

An orthogonal polar network used for modelling of a wearable patch antenna model is presented in Fig. 2, showing a space discretization within the section of a cylinder in  $r$ - $\varphi$  plane. The presented cross-section of the patch antenna also illustrates the correction of the cell dimensions in case of bending so that dimensions of the metallic surfaces and slots remain constant. Actually, mesh resolution is determined in two regions with slightly different values along the angular direction:

- (1)  $\Delta\theta_{patch}$  defined by the bending angle  $2\theta$  in respect to the length of the patch  $l$  ( $2\theta = l / (R+h) = \Delta\theta_{patch} * N_{cells}(patch)$ ), where  $N_{cells}(patch)$  is a number of cells corresponding to the length of radiated patch, and
- (2)  $\Delta\theta_{sub}$  determined according to the condition that the ground length  $L$  remains constant under bending ( $L = R (2\theta + \Delta\theta_{sub} * (N_{cells}(ground) - N_{cells}(patch)))$ ), where  $N_{cells}(ground)$  is a total number of cells corresponding to the length of ground plane.

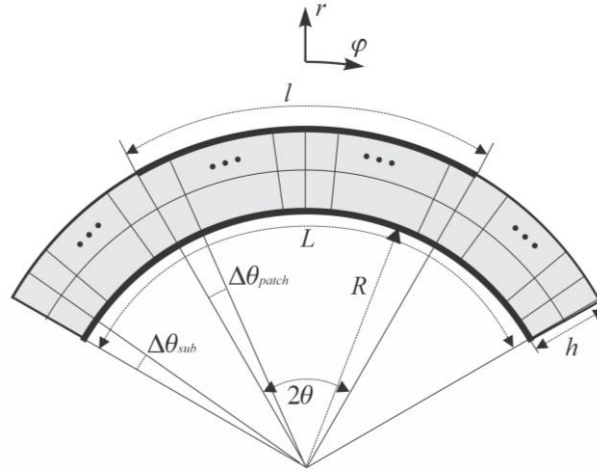


**Fig.2** Space discretization in  $r$ - $\varphi$  plane in a wearable antenna model

The in-house *TLMcyl* solver [20-23] has been used to analyze an impact of the bending on the performances of wearable slotted antenna consisting of the rectangular radiated patch with dimensions  $w \times l = (50 \times 39.5)$  mm, placed on the substrate, and the ground plane of dimensions  $W \times L = (100 \times 100)$  mm [11,21,22]. The antenna is realized on the substrate of the relative permittivity  $\epsilon_r = 2.1 - j 0.001$  (loss tangent  $\sigma = 0.00048$ ) and the height  $h = 2$  mm, and it is bent over a part of a cylinder. A coaxial feed with an inner conductor radius of 0.1 mm, connecting the ground plane to the patch, is positioned 11.5 mm from the patch edge to provide impedance matching with the antenna [21,22].

In the considered model, the muscle tissue of the permittivity  $52.671 - j 13$  (loss tangent  $\sigma = 0.24682$ ) [3,21], and thickness 35 mm is placed beneath the antenna. The reference results of no-slotted antenna were from [21], where the tissue was modeled on the same manner, as homogeneous region with the characteristics of the muscle tissue in terms of permittivity in the complete space under the antenna. Since the antennas were analyzed with a metal ground plane, the inclusion of tissue in the model does not cause significant differences, as confirmed by the results of the rectangular antenna modeling [21,22]. In this particular case, the model included one layer of muscle tissue in order to present the possibility of modeling the influence of the body, which would certainly have greater significance when the antenna structure is different in terms of the ground plane. The cylindrical model is generally well-suited for representing real parts of the human

body, such as the arm, leg, and torso, as a multi-layered structure (skin, fat, muscle, and bone), whose effects can be analyzed in antenna configurations with varying radiation characteristics.

Table 1 presents computational mesh parameters, specifically cell size and the number of cells divided by axis relevant to a cylindrical coordinate system, which are used for modeling of slotted patch antennas on a muscle tissue. Since the patch antenna is considered as an open problem, an appropriate extension around the physical antenna structure is included to form a computational box (represented as padding in the Table 1) allowing for the adequate representation of the antenna surroundings, necessary for the proper capturing of radiation and calculation of the antenna parameters [21,22]. As can be seen, the mesh resolution in the substrate is 1 mm while in other regions the cell size is set to meet time synchronization demands [15]. Note that the same cell size is used for the flat case antenna modeling in a rectangular TLM model, so the total number of cells is equal to presented here for the cylindrical model.

When introducing slots, a defined mesh is completely the same, since the metallic layers are modelled as imprinted onto the substrate via internal boundary conditions (PEC,  $\Gamma=-1$ ), while the cells corresponding to the slots are excluded from defining internal boundary conditions allowing a regular connection and an impulse exchange between neighbouring cells representing the substrate and the air.

In this paper, two slot configurations inserted onto the radiated patch are considered to achieve the tuning effect, as shown in Fig.3:

- octagon-shaped slot composed from square unit elements characterized by parameter  $s$ ,
- U-shaped slot with dimensions characterized by parameters  $s_1$ ,  $s_2$  and  $d$ .

**Table 1** Computational mesh parameters in cylindrical TLM model of slotted wearable antenna under bending

Axis	Medium	Permittivity	Number of cells	Resolution/Cell size
r-axis (height)	muscle	$52.67-j13$	175	$\sim 0.2$ mm
	substrate	$2.1-j0.001$	2	1 mm
	air	1	28	1.45 mm
$\varphi$ -axis (length)	padding	1	28	$(R+h)\Delta\theta_{padd}=1.45$ mm
	substrate	$2.1-j0.001$	30	$\Delta\theta_{sub}=(L/R - l/(R+h))/60$ , $R\Delta\theta_{sub}=1.01$ mm
	substrate/patch	$2.1-j0.001$	39	$\Delta\theta_{patch}=(l/(R+h))/39$ , $(R+h)\Delta\theta_{patch}=1.01$ mm
	substrate	$2.1-j0.001$	30	$\Delta\theta_{sub}=(L/R - l/(R+h))/60$ , $R\Delta\theta_{sub}=1.01$ mm
	padding	1	28	$(R+h)\Delta\theta_{padd}=1.45$ mm
z-axis (width)	padding	1	28	1.45 mm
	substrate	$2.1-j0.001$	25	1 mm
	substrate/patch	$2.1-j0.001$	49	1.02 mm
	substrate	$2.1-j0.001$	25	1 mm
	padding	1	28	1.45 mm

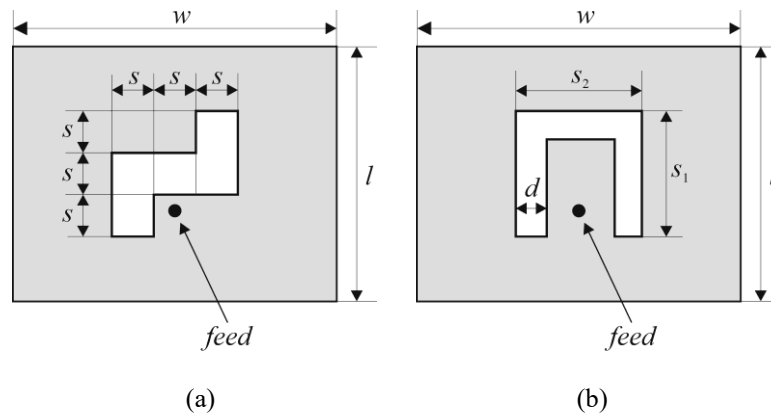


**Fig. 3** Geometry of the antenna element with slot (a) octagon-shaped (b) U-shaped

### 3. SIMULATION RESULTS AND ANALYSES

Simulations using the TLM method are carried out to analyze the influence of the bending on the parameters of slotted wearable antennas. This analysis included both flat and bent antennas with bending angles of 25 and 50 degrees. Results for the flat antenna obtained by the cylindrical and the rectangular TLM mesh, with a 1.0 mm cell size, are compared to verify the accuracy and consistency of the cylindrical TLM method when analysis of slotted antenna parameters is concerned. The comparison aimed to assess the effectiveness of cylindrical TLM model in obtaining the reflection coefficient under flat antenna conditions, providing valuable insights into their applicability for further analysis under bending conditions. In case of the flat antenna model in the cylindrical grid, a very small bending angle of 0.1 degrees is applied, with equivalent radius of the cylinder satisfying the condition  $R \gg l$  (about 500 times) [21,22]. This small angle applied to the antenna model in the cylindrical grid effectively rendered the patch in plane, allowing it to be considered flat for the purposes of the analysis.

The applicability a cylindrical mesh with almost no curvatures to model flat antenna structures has been confirmed in case of a rectangular patch antenna (without slot) [21,22]. As presented in Fig.4, in considered range up to 4.5 GHz that covers two resonances, the values of resonances frequencies - 2.444 GHz and 3.965 GHz, in respect to the corresponding results based on the rectangular mesh - 2.473 GHz and 4.022 GHz, have obtained with small relative errors of 1.17%, and 1.42%, respectively. However, differences in use of rectangular and cylindrical TLM approach for analysis of bent antennas are attributed to the rectangular model that introduces the approximation of curved surfaces, affecting the antenna parameters differently depending on the mesh resolution [21,22]. While the rectangular TLM method requires a fine mesh to reduce approximation errors and provide accurate results regarding the bending influence, the cylindrical approach, using the same mesh resolution as in the flat antenna case, gives reliable results of the frequency shift due to the bending since the mesh consistency is ensured for different angles. Fig.5 presents the results for the bent no-slotted antenna obtained by the cylindrical mesh in the range with two resonances. It can be seen that a larger bending angle results in a larger resonant frequency shifting. Also, a difference can



be observed in terms of a greater effect of bending on frequency shift at the first resonance than at the second one.

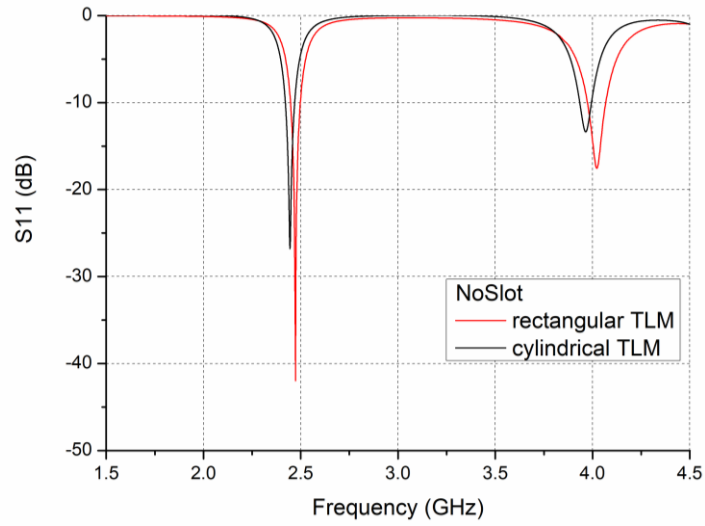


**Fig. 4** The reflection coefficient of the rectangular patch antenna (without slot) for the flat case

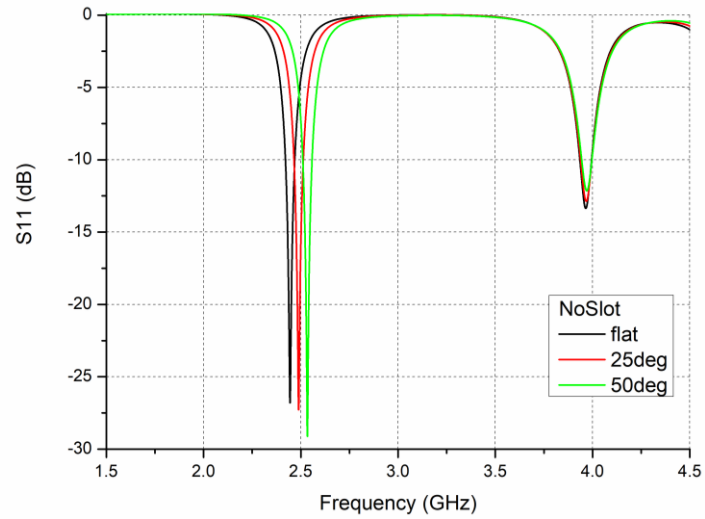


**Fig. 5** The reflection coefficient of the rectangular patch antenna (without slot) under the bending

### 2.1. A Patch Antenna with a Octagon-shaped Slot

First antenna model with different dimensions of octagon-shaped slot, as shown in Fig 3(a), is designed using the TLM cylindrical mesh using the 1.0 mm cell size. The octagon-shaped slot with two different dimensions of a unit square element  $s = 3$  mm and  $s = 5$  mm is embedded into the radiated patch surface.

To verify the model, comparison of simulated results, representing the reflection coefficient obtained by the cylindrical and the rectangular TLM mesh, for the cases of a flat antenna with a octagon slot, are shown in Fig.6. Comparison of resonant frequencies is presented in Table 2. There is a good agreement between results reached via the cylindrical mesh and the corresponding rectangular mesh results. Moreover, resonant frequency tuning by changing the slot dimensions is illustrated.

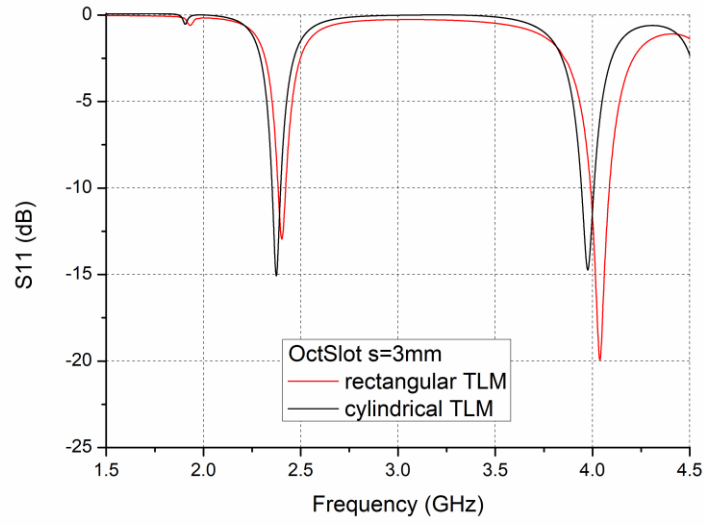
**Table 2** Comparison of results of resonant frequencies for the flat case with an octagon-shaped slot consisted of 5 square elements of dimension  $s$

Octagon slot size	Resonant frequencies [GHz]		Relative Error
	cylindrical	rectangular	
	TLM	TLM	
$s = 3$ mm	2.374	2.403	1.19 %
	3.975	4.038	1.52 %
$s = 5$ mm	2.226	2.254	1.23 %
	3.959	4.029	1.73 %

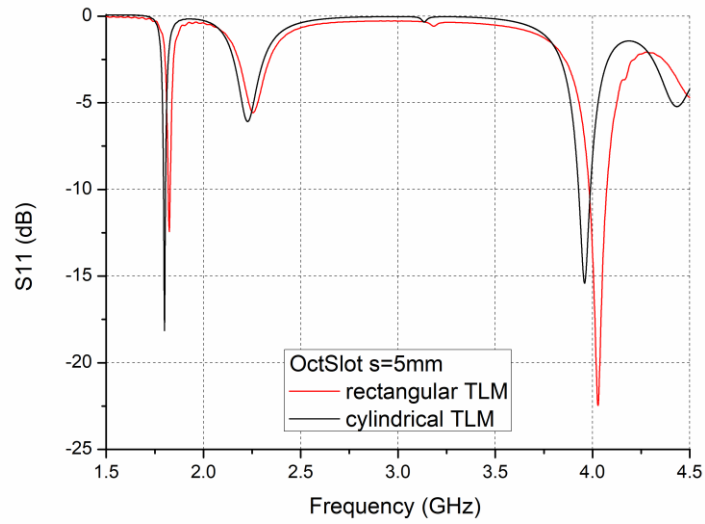
In order to investigate the influence of the bending on antenna parameters, the slotted antenna is bent over a part of cylinder to achieve the bending angles of 25 and 50 degrees. Fig.7 shows simulated results obtained for two different bending angles compared with the flat case. As can be seen, the first resonance is significantly more affected than the second one when the antenna is bent, with the frequency going up with an increase of the bending angle, while the second resonance remains almost the same.

Fig.8 presents a summary how introducing the slot and the slot size affects antenna parameters under flat or bending conditions. The influence of the octagon-shaped slot is seen in the shifting of frequencies to lower values. Furthermore, increasing the size of the slot additionally reduces the frequencies. Note that these affects are much more pronounced for the first resonance. Finally, there is an agreement between the resonant frequency and reflection coefficient values with the corresponding results reached via the rectangular mesh for the case of the flat antenna.

In addition, the antenna radiation patterns at the frequency of the first resonance for both considered cases of octagon slot dimensions, compared to the no-slotted antenna, are plotted in Fig. 9. It can be observed that inserting an octagon slot in the antenna does not cause significant changes in the radiation patterns compared to the no-slot case. Also, the back region of the slotted antenna's radiation pattern shows an increase in gain with increasing slot dimension.

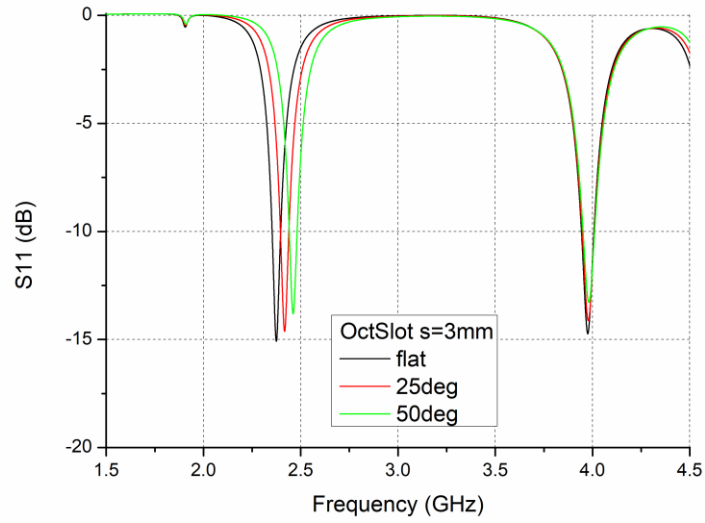


(a)

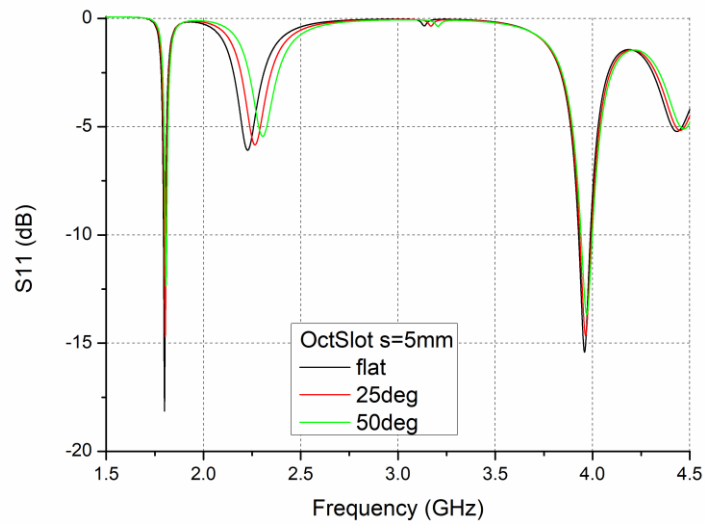


(b)

**Fig. 6** The reflection coefficient of the slotted patch antenna for the flat case with an octagon-shaped slot consisted of 5 square elements of dimension  $s$  (a) 3 mm, (b) 5 mm.



(a)



(b)

**Fig. 7** The reflection coefficient of the slotted patch antenna under the bending for the octagon-shaped slot consisted of 5 square elements of dimensions (a)  $s = 3$  mm, (b)  $s = 5$  mm.

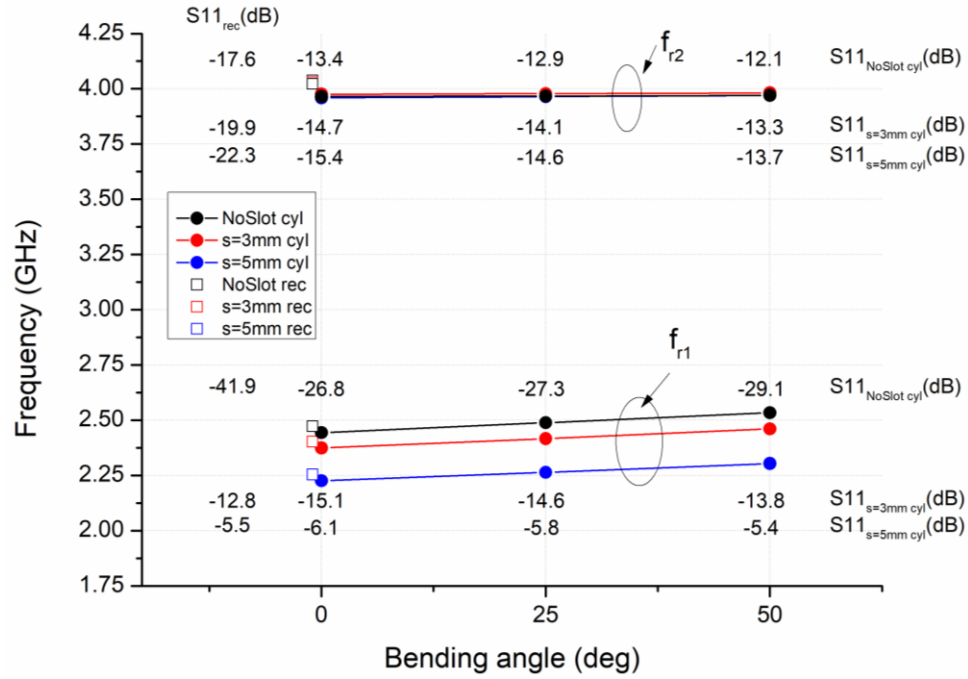


Fig. 8 The antenna parameters versus bending angle for different octagon-slot dimensions.

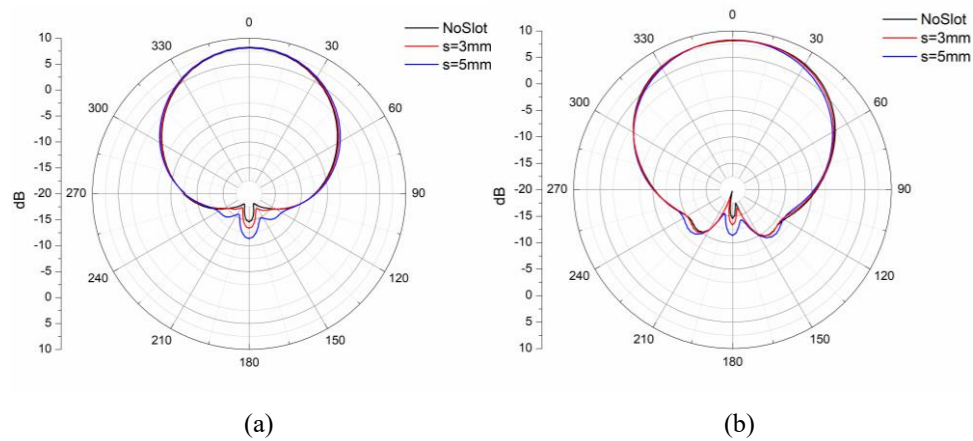


Fig. 9 Comparison of the radiation intensity of the slotted antenna with different octagon slot dimensions and the no-slotted antenna in the cross-section along (a) the  $r-\phi$  plane (E-plane) and (b) the  $r-z$  plane (H-plane).

## 2.2. A Patch Antenna with an U-shaped slot

Another antenna structure considered here contains the U-slotted patch geometry shown in Fig 3(b). The TLM method based on the cylindrical mesh with 1.0 mm cell size is used applied for antenna modelling. Initially, the antenna model with slot dimensions  $s_1 = s_2 = 15\text{mm}$ ,  $d = 1\text{mm}$ , is considered. After that, the size of the slot is increased by  $d = 2\text{mm}$  toward the inside of the U-shaped slot by maintaining constant values of  $s_1 = s_2 = 15\text{mm}$ .

Fig.10 shows the comparison of reflection coefficient obtained by the cylindrical and the rectangular grid, in cases of the flat antenna with embedded U-slot configurations. A good agreement of the results obtained by applying two different meshes is achieved. The corresponding results of resonant frequencies compared in terms of accuracy are presented in Table 3. Also, as it is shown from Fig.10, the resonant frequency, as well as the  $S_{11}$  parameter is changed due to variations of the U-slot dimensions.

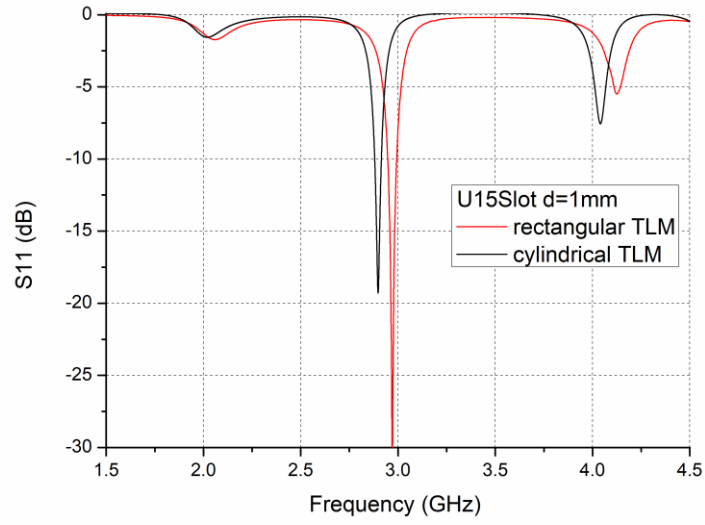
Simulated results for considered U-slotted patch configurations, showing the effect of bending on the resonant frequencies, are presented in Fig.11. As expected, increasing the bending angle makes resonant frequencies to rise. Also, there is a greater effect of the bending on the first resonance than on the second one for the bent antenna.

**Table 3** Comparison of results of resonant frequencies for the flat case with an U-slotted patch antenna for the flat case with slot dimensions  $s_1 = s_2 = 15\text{ mm}$  and  $d$

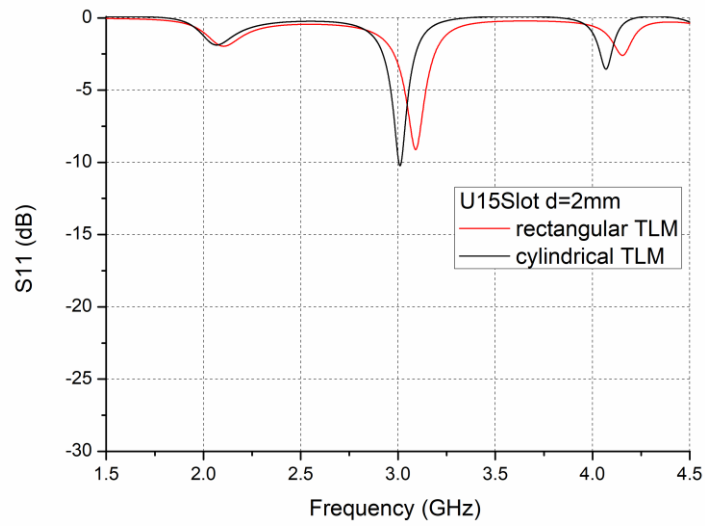
U slot size	Resonant frequencies		Relative Error
	[GHz]		
	cylindrical TLM	rectangular TLM	
$d = 1\text{ mm}$	2.897	2.970	2.44 %
	4.040	4.125	2.04 %
$d = 2\text{ mm}$	3.010	3.090	2.57 %
	4.069	4.150	1.94 %

Fig.12 shows a review of the bending influence on parameters of U-shaped slotted antenna, for bending angles of 25 and 50 degrees, together with a flat case antenna, and a comparison with the rectangular model results. In contrast to the octagon-shaped slot, it can be concluded that the U slot size affects both frequencies to rise in respect to rectangular antenna.

The radiation patterns for the U-shaped slotted antenna dimensions are compared to the antenna without slot in Fig. 13. In comparison with the octagon slot, it can be seen that the radiation pattern is more significantly affected when the U-shaped slot is inserted. The plots show that the pattern becomes broader as the slot dimension increases, along with a slight decrease in gain in the main lobe. On the other hand, the back region of the radiation pattern shows an increase in gain compared to the no-slotted antenna. This decrease in front-to-back ratio may be of interest in BME applications, as it indicates reduced anisotropy in radiation patterns when the antenna is applied to dynamic bodies or objects, as well as in antenna-body interactions.

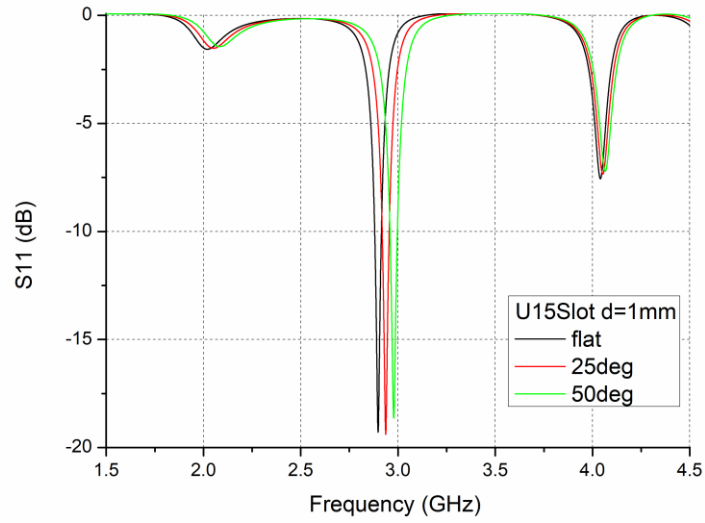


(a)

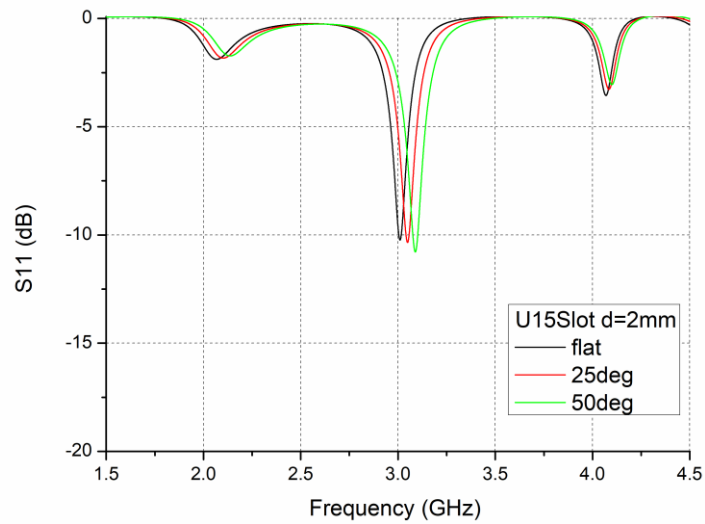


(b)

**Fig. 10** The reflection coefficient of the U-slotted patch antenna for the flat case with slot dimensions  $s_1 = s_2 = 15$  mm and (a)  $d = 1$  mm, (b)  $d = 2$  mm



(a)



(b)

**Fig. 11** The reflection coefficient of the U-slotted patch antenna for the bent antenna with slot dimensions  $s_1 = s_2 = 15$  mm and (a)  $d = 1$  mm, (b)  $d = 2$  mm



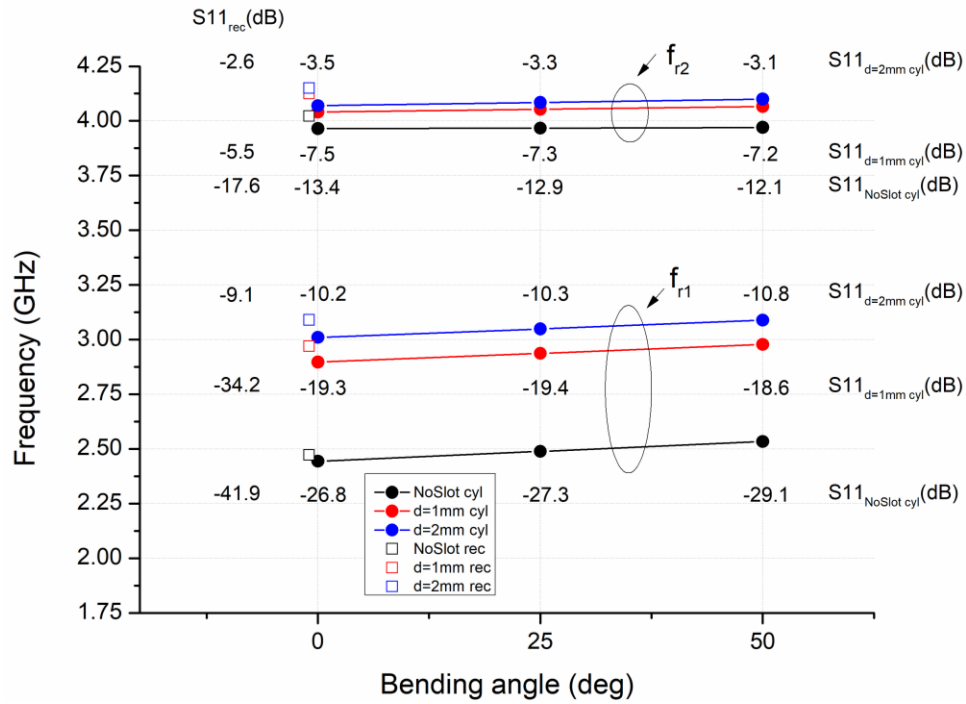


Fig. 12 The antenna parameters versus bending angle for different U-slot dimensions

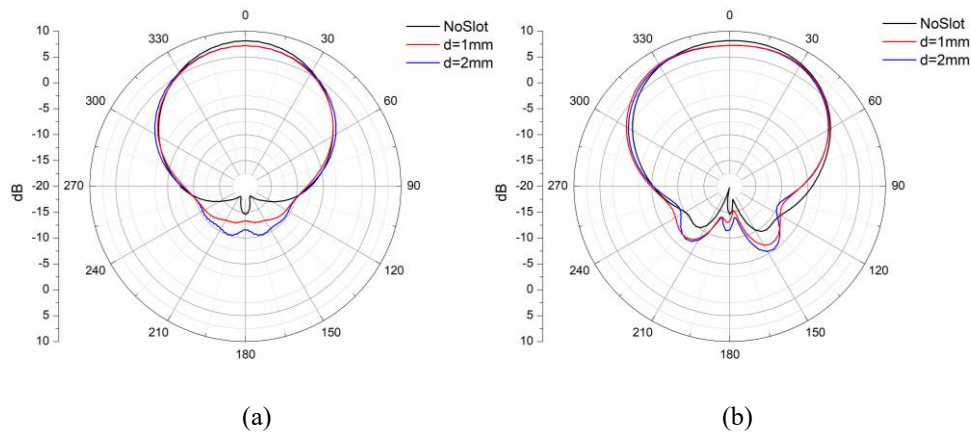


Fig. 13 Comparison of the radiation intensity of the antenna with U-slot for different dimensions with the no-slotted antenna, in cross-section along (a)  $r-\phi$  plane (E-plane), and (b) in  $r-z$  plane (H-plane).

#### 4. CONCLUSION

This paper demonstrates the capabilities of the cylindrical TLM solver for analyzing wearable patch antennas featuring radiating patches with complex geometries, including polygon-shaped and U-shaped slots. Model validation is carried out for the flat antenna case by comparing the results with those obtained using a rectangular TLM mesh. By illustrating the effects of slot shape and dimensions on the shifting of resonant frequencies, as well as changes in the reflection coefficient and radiation patterns, the presented results confirm the importance of accurate slot modeling.

The slotted antenna model, based on a cylindrical mesh conformal to various bending angles, enables comprehensive and precise analysis of the influence of slot shape and dimensions on resonant behavior, while also incorporating the effects of antenna bending. Limitations of the model, related to representing slot shapes and dimensions in accordance with the cell network resolution, can be addressed through the introduction of compact slot models, which will be explored in future work.

**Acknowledgement:** *This work has been supported by the Ministry of Science, Technological Development and Innovation of the Republic of Serbia [grant number 451-03-137/2025-03/ 200102].*

#### REFERENCES

- [1] J. Jokovic, T. Dimitrijevic, A. Atanaskovic and N. Doncov, "Wearable Slotted Antenna Modelled by Cylindrical TLM Method", In Proceedings of the 16th International Conference on Advanced Technologies, Systems and Services in Telecommunications (TELSIKS), Niš, Serbia, pp. 360-361, 2023.
- [2] H. Yang and X. Liu, "Wearable Dual-Band and Dual-Polarized Textile Antenna for on- and Off-Body Communications", *IEEE Antennas Wireless Propag. Lett.*, vol. 19, no. 12, pp. 2324-2328, 2020.
- [3] C. X. Mao, D. Vital, D. H. Werner, Y. Wu and S. Bhardwaj, "Dual-Polarized Embroidered Textile Armband Antenna Array With Omnidirectional Radiation for on-/Off-Body Wearable Applications", *IEEE Trans. Ant. Prop.*, vol. 68, no. 4, pp. 2575-2584, 2020.
- [4] Y. L. Chow, Z. N. Chen, K. F. Lee and K. M. Luk, "A Design Theory on Broadband Patch Antennas With Slot", In Proceedings of IEEE Antennas Propag. Soc. Int. Symp. Dig., Atlanta, USA, Jun. 1998, vol. 2, pp. 1124-1127.
- [5] S. Xiao, B. Z. Wang and X. S. Yang, "A Novel Frequency Reconfigurable Patch Antenna", *Microwave Opt. Tech. Lett.*, vol. 36, pp. 295-297, 2003.
- [6] Y. Chen and C. F. Wang, "Characteristic-Mode-Based Improvement of Circularly Polarized U-Slot and E-Shaped Patch Antennas", *IEEE Antennas Wireless Propag. Lett.*, vol. 11, pp. 1474-1477, 2012.
- [7] K.-F. Lee, S. L. S. Yang and A. A. Kishk, "Dual- and Multiband U-Slot Patch Antennas", *IEEE Antennas Wireless Propag. Lett.*, vol. 7, pp. 645-647, 2008.
- [8] F. Yang, X.-X. Zhang, X. Ye and Y. R. Samii, "Wide-Band E-Shaped Patch Antennas for Wireless Communications", *IEEE Trans. Ant. Propag.*, vol. 49, no. 7, pp. 1094-1100, 2001.
- [9] E. K. Kaivanto, M. Berg, E. Salonen and P. de Maagt, "Wearable Circularly Polarized Antenna for Personal Satellite Communication and Navigation", *IEEE Trans. Antennas Propag.*, vol. 59, no. 12, pp. 4490 - 4496, Dec. 2011.
- [10] A. Khidre, K.-F. Lee, A. Z. Elsherbeni and F. Yang, "Wide Band Dual-Beam U-Slot Microstrip Antenna", *IEEE Trans. Ant. Propag.*, vol. 61, no. 3, pp. 1415-1418, Mar. 2013.
- [11] L. Song and Y. Rahmat-Samii, "A Systematic Investigation of Rectangular Patch Antenna Bending Effects for Wearable Applications", *IEEE Trans. Ant. Prop.*, vol. 66, no. 5, pp. 2219-2228, 2018.
- [12] K. S. Kunz and R. J. Luebbers, *The Finite Difference Time Domain Method for Electromagnetics*, CRC Press, Boca Raton, FL, 1993.
- [13] W.C. Gibson, *The Method of Moments in Electromagnetics*, Chapman and Hall/CRC, 2021.
- [14] T.J.R. Hughes, *The Finite Element Method: Linear Static and Dynamic Finite Element Analysis*, Prentice-Hall, 1987.

- [15] C. Christopoulos, *The Transmission-Line Modelling Method: TLM*, Institute of Electrical and Electronics Engineers, 1995.
- [16] O. Messaoudi, O. Beneyello, D. Pompei and A. Papiernik, "The Transmission Line Matrix Method Applied to Microstrip Antennas", In Proceedings of 1988 AP-S Digest, 1988, pp. 1022-1025.
- [17] N. Fichtner, U. Siart, Y. Kuznetsov, A. Baev and P. Russer, "TLM Modeling and System Identification of Optimized Antenna Structures", *Adv. Radio Sci.*, vol. 6, pp. 45-48, 2008.
- [18] S. Ghosh, S. Chatterjee and B. Gupta, "Meander-Lined Implantable Antenna Design at 2.45 GHz Using Transmission Line Model", *IETE J. Res.*, vol. 70, no. 11, pp. 8127-8139, 2024.
- [19] T. Dimitrijević, J. Joković, B. Milovanović and N. Dončov, "TLM Modeling of a Probe-Coupled Cylindrical Cavity Based on Compact Wire Model in the Cylindrical Mesh", *Int. Jour. of RF and Microw. Comp.-Aided Eng.*, vol. 22, no. 2, pp. 184-192, 2012.
- [20] T. Dimitrijević, J. Joković and N. Dončov, "Efficient Modelling of a Circular Patch-Ring Antenna Using the Cylindrical TLM Approach", *IEEE Antennas and Wireless Propag. Lett.*, vol. 16, pp. 2070-2073, Apr. 2017.
- [21] J. Joković, T. Dimitrijević, A. Atanasković and N. Dončov, "Computational Modeling of the Bent Antenna in an On-Body Mode Using the Cylindrical TLM Approach", *Math. Probl. Engineer.*, vol. 2022, p. 8486740, 2022.
- [22] T. Dimitrijević, A. Vuković, A. Atanasković, J. Joković, P. Sewell and N. Dončov, "Holistic Analysis of Conformal Antennas Using the Cylindrical TLM Method", *IEEE Trans. Ant. Propag.*, vol. 71, no. 5, pp. 4028-4035, 2023.
- [23] J. Joković, T. Dimitrijević, N. Dončov and B. Milovanović, "Efficient Integral Cylindrical Transmission Line Matrix Modelling of a Coaxially Loaded Probe Coupled Cavity", *IET Microwaves, Ant. & Prop.*, vol. 9, no. 8, pp. 788-794, 2015.